TuijinJishu/Journal of Propulsion Technology
ISSN: 1001-4055
Vol. 44 No. 3 (2023)

Multivariate Analysis of Prandtl, Reynolds, and Richardson Numbers in Lid-Driven Cavity Flow

Abu Fahad[1], Deep Parkash Singh[2], Ankush Gaurav[2], Hemant Kumar Singh[2], Navin Chaurasiya[2], Sandip Kumar Singh[3], Aparna Singh Gaur[4]

[1] *Research Scholar, Department of Mechanical Engineering, Veer Bahadur Singh Purvanchal University, Jaunpur, India*

[2] *Assistant Professor, Department of Mechanical Engineering, Veer Bahadur Singh Purvanchal University, Jaunpur, India*

[3] *Assistant Professor, Department of Mechanical Engineering, Veer Bahadur Singh Purvanchal University, Jaunpur, India*

[4] *Lecturer, Department of Mechanical Engineering, Savitri Bai Phule Government Polytechnic, Azamgarh, India*

Abstract:-This study presents Direct Numerical Simulations (DNS) of a two-dimensional lid-driven cavity flow, investigating the influence of heating of the bottom wall and movement of the top lid on the flow characteristics. The simulations are performed at Reynolds numbers (Re) of 500, 1000, 2500, 5000, and 10000, and Prandtl numbers (Pr) of 0.03, 0.72, 7.1, and 100 using different working fluids, namely mercury, air, water, and glycerol. The sidewalls of the enclosure are considered adiabatic, while the bottom wall is heated, and the top plate is kept at a lower temperature. Validation of the developed numerical code is performed by comparing the results with Ghia et al. for the non-heating case and Moallemi et al. for the heating case. Temperature and streamline profiles are obtained for various Richardson numbers (Ri) ranging from 0 to 30 for Re values of 500, 1000, 2500, 5000, and 10000, where Ri represents the ratio of buoyancy effects to viscous effects and is varied to examine low and moderate magnitudes within the limits of the Boussinesq approximation.The investigation of the time-averaged drag reveals its dependency on Richardson numbers for the range of Ri=0 to Ri=100, considering Re values of 500, 1000, 2500, 5000, and 10000.The findings from this study provide valuable insights into the thermal and dynamic behavior of lid-driven cavity flows with varied heating and movement effects, contributing to a better understanding of convective heat transfer and fluid motion in similar engineering and natural systems.

Keywords*:Lid-driven cavity, Computational Fluid Dynamics, Navier-Stokes equations, diesel-ethanol blends..*

1. Introduction

The lid-driven cavity is a well-established benchmark problem in Computational Fluid Dynamics (CFD) for evaluating numerical solutions of the Navier-Stokes equation. It has various applications in electronic devices, lubrication technologies, chemical processing equipment, and drying technologies. The cavity consists of four walls, with one wall moving at a constant velocity and the others stationary. When the cavity walls have different temperatures, mixed convection occurs due to the combined effect of shear from the moving wall and natural convection. This study reviews existing research on lid-driven cavity flows and aims to identify gaps in the current understanding. Several papers have investigated different aspects of the problem. Quere et al. (Reference [1]) used Chebyshev polynomials to compute natural convection in a differentially heated cavity

with air as the working fluid. Cardenas et al. (Reference [2]) employed the finite volume method to examine various cavity geometries at different Reynolds numbers. Koseff et al. (Reference [3]) studied the flow in athree-dimensional lid-driven cavity using flow visualization and velocity and heat flux measurements. Venugopal et al. (Reference [4]) investigated vortical flow structures in low and high Reynolds number lid-driven cavities using computational simulations. Kothuru et al. (Reference [5]) numerically studied micropolar fluid flow in a lid-driven square cavity. Moallemi et al. (Reference [6]) analyzedPrandtl number effects on mixed convection heat transfer in a lid-driven cavity. Thakera (Reference [7]) performed numerical simulations of isothermal flow patterns in various lid-driven cavity configurations using OpenFOAM. Singh (Reference [8]) focused on mixed convection in a lid-driven square cavity for different Richardson numbers. Mukherrjee (Reference [9]) conducted Direct Numerical Simulations of a two-dimensional lid-driven cavity at specific Reynolds and Prandtl numbers. This review identifies some unexplored areas, such as investigating mixed convection in more diverse cavity geometries, examining unsteady flow patterns, and exploring the effects of additional parameters. Future research can delve into these aspects to enhance our understanding of lid-driven cavity flows and their practical applications in diverse engineering and technological fields.

2. Methodology

2.1 Problem Definition

In the present work the geometry is considered to be a square cavity i.e. aspect ratio is of the order of unity. As the problem is in two dimensions, the length of the geometry perpendicular to the plane is assumed to be very long in the third dimension. The geometry of the cavity is as shown below:

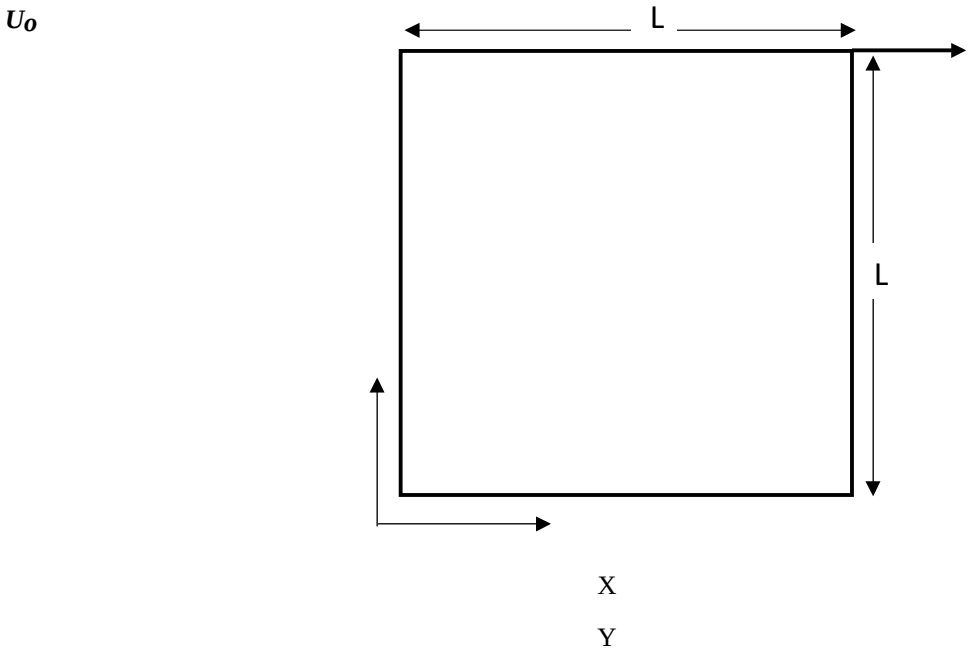

Fig 2.1 a schematic diagram of Lid driven cavity

The top wall is moving in the positive x direction with a constant velocity Uo and all the three walls are stationary. All the walls are at certain reference temperatures. The cavity is filled with water. The thermo physical properties of water is assumed to be constant except the density which varies according to Boussinesq approximation. Water is assumed to be Newtonian and incompressible.

2.2 Mathematical Model

In this study, we utilize a mathematical model grounded in the principles of fluid mechanics and heat transfer to accurately simulate the dynamic behavior of diverse fluids within a lid-driven cavity. The fundamental

governing equations encompass the continuity equation, Navier-Stokes equations, and energy equation. These equations are effectively solved through the application of computational fluid dynamics (CFD) methodologies

2.3 Governing Equations

The continuity equation represents the conservation of mass and is given by:

$\nabla \cdot (\rho u) = 0,$

where ρ is the density and u is the velocity vector.

The Navier-Stokes equations, which describe the conservation of momentum, are expressed as:

$\rho(\partial u/\partial t + u \cdot \nabla u) = -\nabla P + \mu \nabla^2 u + \rho g,$

where P is the pressure, μ is the dynamic viscosity, and g represents the gravitational acceleration.

The energy equation considers the conservation of energy and is given by:

$\rho Cp(\partial T/\partial t + u \cdot \nabla T) = \nabla \cdot (k\nabla T) + Q,$

whereCp is the specific heat capacity, T is the temperature, k is the thermal conductivity, and Q represents the heat source/sink term.

2.4 Computational Fluid Dynamics (CFD)

The numerical simulations are performed using a commercial CFD software package. The software utilizes finite volume methods to discredited the governing equations and solve them iteratively in a computational domain representing the lid-driven cavity. The flow and thermal properties of the diesel-ethanol blends are computed at each grid point within the domain.

2.5 Boundary Conditions

The simulation of the lid-driven cavity involves the definition of boundary conditions. The upper boundary signifies the lid in motion, for which a designated velocity profile is stipulated. The other boundaries are treated as solid walls, subject to no-slip conditions, ensuring their immobility. Inlet and outlet boundaries are thoughtfully positioned to sustain a self-contained and recirculation flow within the cavity. Temperature boundary conditions are carefully established to emulate the thermal attributes inherent to the system

2.6 Numerical Solution

The established governing equations, guided by the specified boundary conditions, are numerically addressed through an iterative algorithm until a converged solution is achieved. The discredited equations are tackled in a progressive time-marching fashion, enabling the exploration of both transient behaviours and steady-state scenarios. Convergence of the numerical solution is gauged against predetermined residual thresholds or stability benchmarks. In order to ensure the fidelity and robustness of the findings, an examination of grid independence is undertaken, involving systematic variations in grid resolution to confirm the constancy of outcomes. Additionally, sensitivity analyses are conducted to delve into the impacts of numerical parameters, including time step size and turbulence modeling, on the simulation outcomes.

3. Validation

The non-uniform grid has been developed and tested for 100*100 points to 150*150. The code has been validated with the benchmark results of Ghia et al .

3.1 Non Heating Case

for the non- heating case i.e. the validation of the momentum equations with the solutions of Ghia et al. for Re=100 and Re=1000.

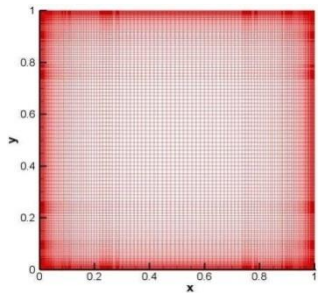

Fig 3.1 (a) Representative meshes employed in validation of the model with Ghia et al.(1982)

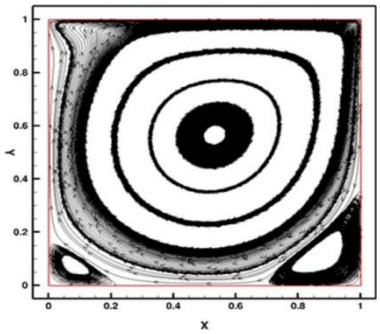

Fig:- 3.1 (b) Streamlines from Ghia et al Fig:- 3.1 (c)Streamlines from present configuration at Re=1000

configuration at Re=1000

3.2 Heating Case

Code validation is conducted by comparing our simulation results with a benchmark numerical solution presented in the work titled 'Prandtl Number Effects on Laminar Mixed Convection Heat Transfer in a Lid-Driven Cavity' by Moallemi et al. (1991). We scrutinize the validity of our model by comparing streamline plots and isotherms across varying Reynolds numbers, Richardson numbers, and Prandtl numbers. The outcomes of this validation are showcased below

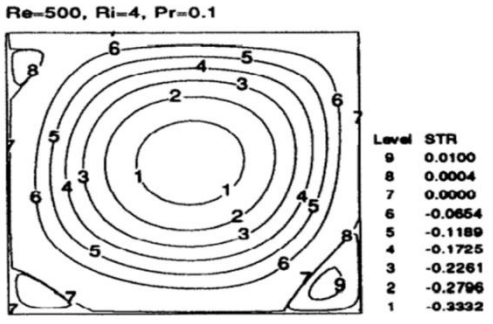

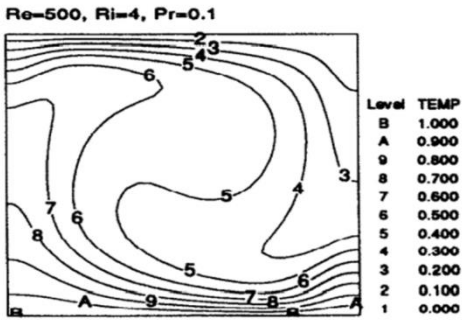

Fig:-3.2 (a) Streamlines and Isotherms contours from Moallemi et al. configuration (Re=500, Ri=4, Pr=0.1)

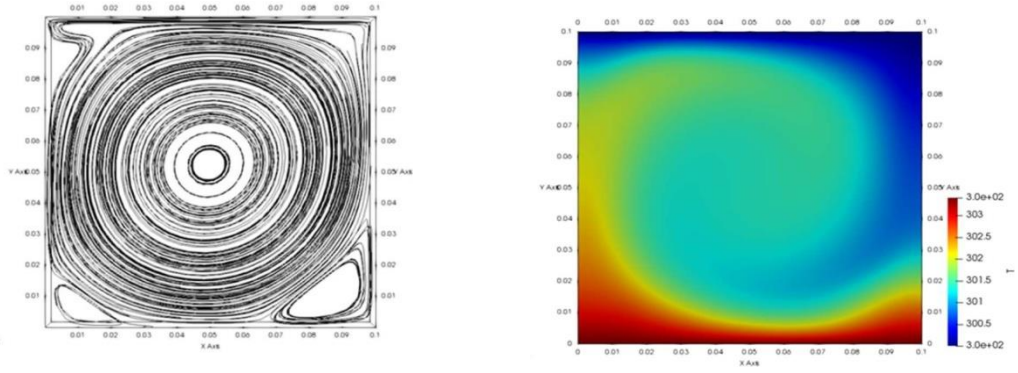

Fig:-3.2 (b) Streamlines and Isotherms contours from present configuration (Re=500, Ri=4, Pr=0.1)

3.3 Validation Parameters

To ensure the accuracy of our numerical simulations, we utilize validation parameters based on Ghia's approach. These parameters encompass velocity profiles, recirculation zones, and relevant flow and thermal characteristics within the lid-driven cavity. We quantitatively or qualitatively compare our simulated results with experimental data to validate our numerical model. This involves a comprehensive analysis of various validation parameters, focusing on consistency and reliability. Sensitivity analyses may also be performed to explore the influence of different modelling assumptions or parameters on the simulation results.

4. Results and Discussion

4.1 Grid Independence Study

The outcome of a CFD simulation can be influenced by the resolution of the computational mesh. To demonstrate the absence of this dependency, a grid independence analysis is conducted. If, upon mesh refinement, the results exhibit minimal variation and progressively converge towards a consistent value, it indicates grid independence within the domain. In our current investigation, CFD simulations were executed on three distinct non-uniform meshes, featuring fine grids along the walls, specifically at resolutions of 100x100, 125x125, and 150x150."

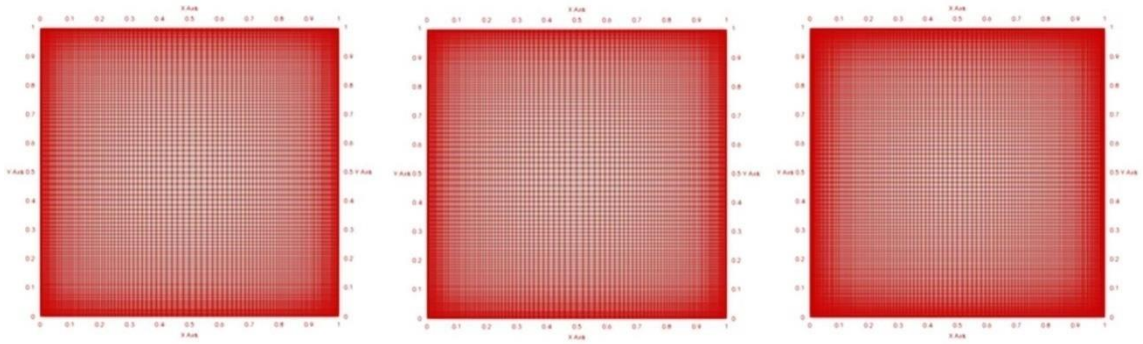

Fig:- 100x100 Non-uniform grids **Fig:-125x125 Non-uniform grids** **Fig:-150x150 Non-uniform grids**

Convergence assessment was conducted by monitoring the dimensionless 'U' velocity values over time at a designated point 'D' within the cavity for RE=500 and Ri=2, 30, 100, as depicted below. The graph demonstrates that the 'U' velocity values nearly reached convergence for both 125x125 and 150x150 non-uniform grids, affirming grid independence. Consequently, based on the successful grid independence test, subsequent research and CFD simulations were pursued utilizing 125x125 non-uniform grids with fine resolutions at the walls. Following the validation of the code against Ghia and Moallemi's benchmark results, the analysis delves into various scenarios, as detailed in section 3.5. To comprehensively cover the cavity, we selected five distinct

points, strategically positioned within the domain. Placing probes at these locations facilitates a holistic understanding. Our objective is to capture the complete cavity behaviour. We evaluate the time histories of 'u' velocity, 'v' velocity, and temperature at these five points.

4.2 Discussion

Streamline plots with instantaneous temperature distribution contours and graphs of time histories of ‘u’ velocity at point D inside the cavity for Re=100, 1000, at Pr=0.03, 0.71,7,100 are shown below. In present study the simulations is performed up to dimensionless time 1000 and the time step is taken as 5-4

Reynolds number=100

Pr=0.03 **Pr=0.71**

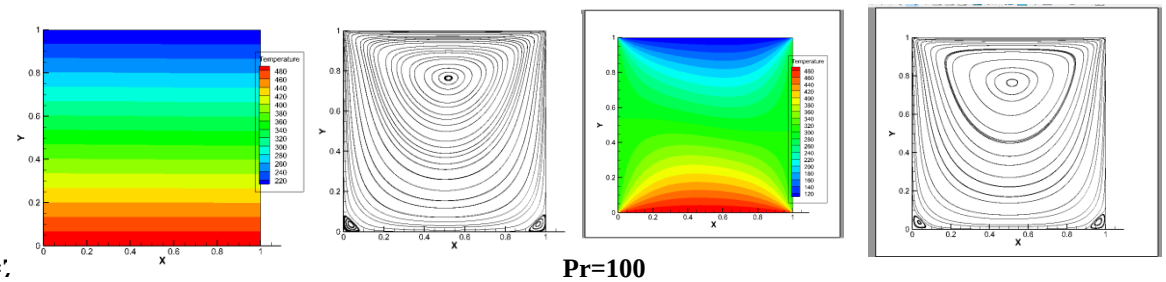

Pr=7 **Pr=100**

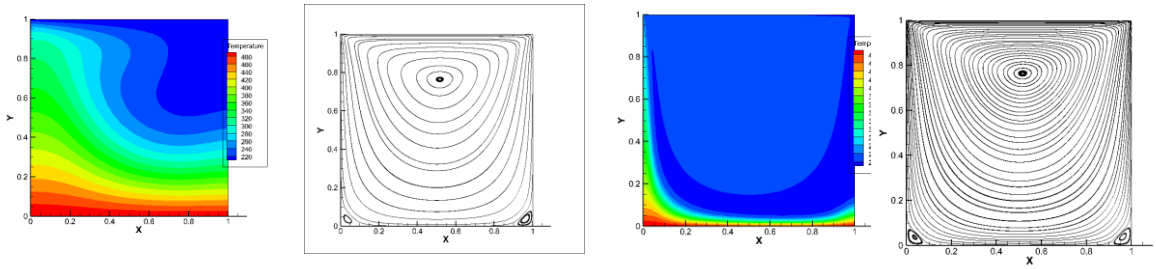

Fig:- Snapshot of Instantaneous Temperature distribution with streamlines inside the cavity at Pr=0.03, Pr=0.71, Pr=7, Pr=100,

The temperature contour with streamline from Pr=0 to Ri=100 for Re=500 is shown above. Due to the motion of the top plate, a vortex is formed which we denote as ‘shear roll’ and due to heating of the bottom plate a vortex is formed which we denote as ‘buoyancy roll’.

In these cases, shear roll is dominating inside the cavity and it is a clockwise vortex. Beside this shear vortex, one anticlockwise vortex is also formed in left side of the bottom plate from Pr=0 to Pr=100. Temperature variation inside the cavity is also shown which shows that at the core temperature variation is negligible and fluid inside the cavity is not well mixed in case of Pr=0. As the Prandtl number increases from Pr=0 to Pr=100, temperature variation has increased slightly that can be seen inside the core which shows, the fluid has now started mixing. Also the vortex formed on bottom left side of the cavity has now goes on decreasing significantly as Prandtl number increases from Pr=0 to Pr=100.

Reynolds number=1000

Pr=0.03 **Pr=0.71**

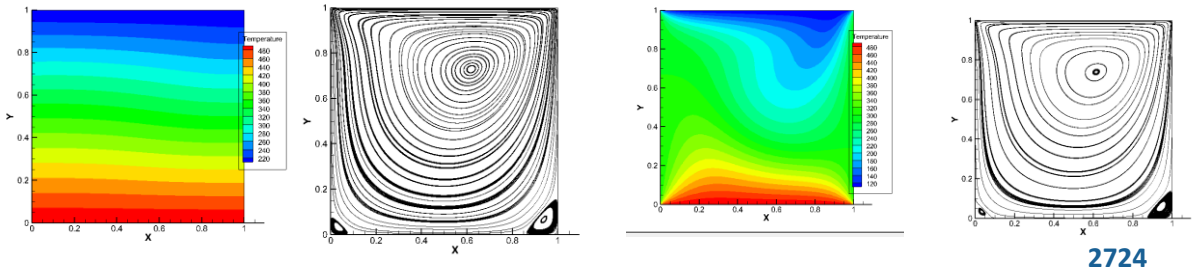

Pr=7 **Pr=100**

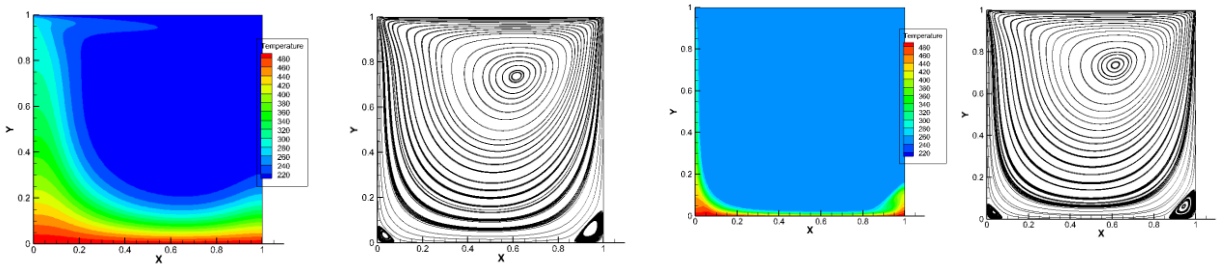

Fig:- Snapshot of Instantaneous Temperature distribution with streamlines inside the cavity at Pr=0.03, Pr=0.71, Pr=7, Pr=100,

The temperature contour with streamline from Ri=0 to Ri=4 for Re=1000 is shown above. In these cases, shear roll is dominating inside the cavity and it is a clockwise vortex. Beside this shear vortex, one anticlockwise vortex is also formed in left side of the bottom plate from Ri=0 to Ri=1 which have now disappeared in case of Ri1 and Ri=2. A secondary vortex on right bottom side of the cavity have now emerged in case of Ri=4. Temperature variation inside the cavity is also shown which shows that at the core temperature variation is negligible and fluid inside the cavity is not well mixed in case of Ri=0. As the Richardson number increases from Ri=0 to Ri=4, temperature variation has increased slightly that can be seen inside the shear roll which shows that fluid has now started mixing.

Streamline plots with instantaneous temperature distribution contours and graphs of time histories of 'u' velocity at point D inside the cavity for Re=500, 1000, 2500, 5000, 1000 at Ri=0, 0.4, 0.8, 1, 2, 4, 5, 10, 12, 15, 25, 30 are shown below. In present study the simulations is performed up to dimensionless time 1000 and the time step is taken as 5-4

Reynolds number=500

Ri=0 **Ri=0.4** **Ri=0.8**

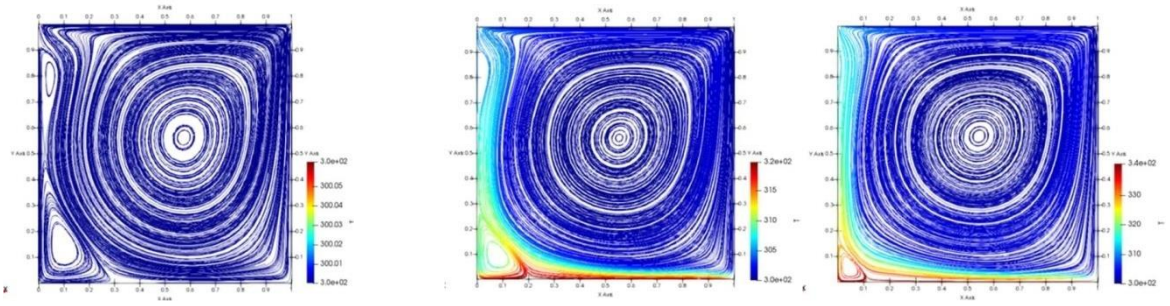

Ri=1 **Ri=2** **Ri=4**

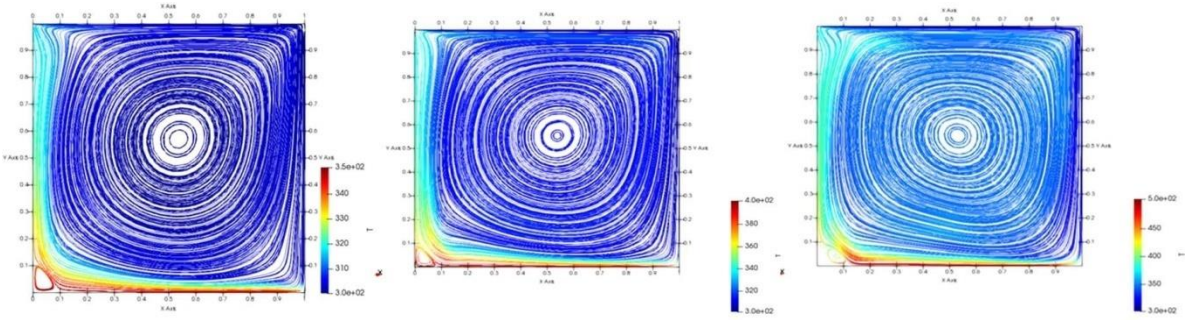

Fig:- Snapshot of Instantaneous Temperature distribution with streamlines inside the cavity at Ri=0, Ri=0.4, Ri=0.8, Ri=1, Ri=2, Ri=4

The temperature contour with streamline from Ri=0 to Ri=4 for Re=500 is shown above. Due to the motion of the top plate, a vortex is formed which we denote as 'shear roll' and due to heating of the bottom plate a vortex is formed which we denote as 'buoyancy roll'.

In these cases, shear roll is dominating inside the cavity and it is a clockwise vortex. Beside this shear vortex, one anticlockwise vortex is also formed in left side of the bottom plate from Ri=0 to Ri=4. Temperature variation inside the cavity is also shown which shows that at the core temperature variation is negligible and fluid inside the cavity is not well mixed in case of Ri=0. As the Richardson number increases from Ri=0 to Ri=4, temperature variation has increased slightly that can be seen inside the core which shows, the fluid has now started mixing. Also the vortex formed on bottom left side of the cavity has now goes on decreasing significantly as Richardson number increases from Ri=0 to Ri=4.

Reynolds number=1000

Ri=0 **Ri=0.4** **Ri=0.8**

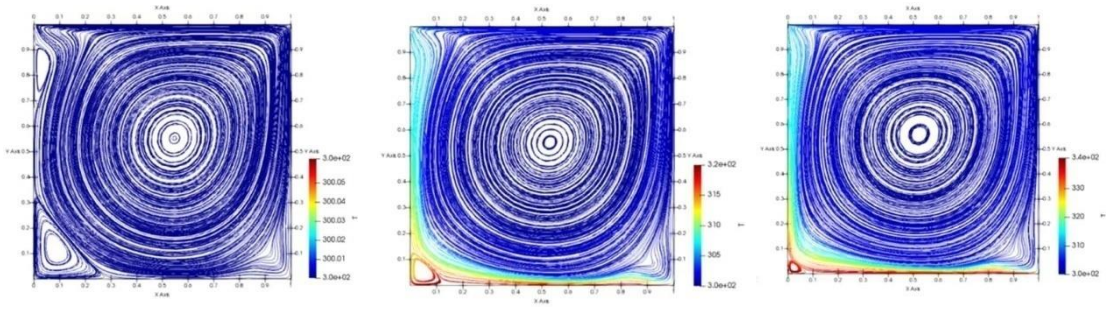

Ri=1 **Ri=2** **Ri=4**

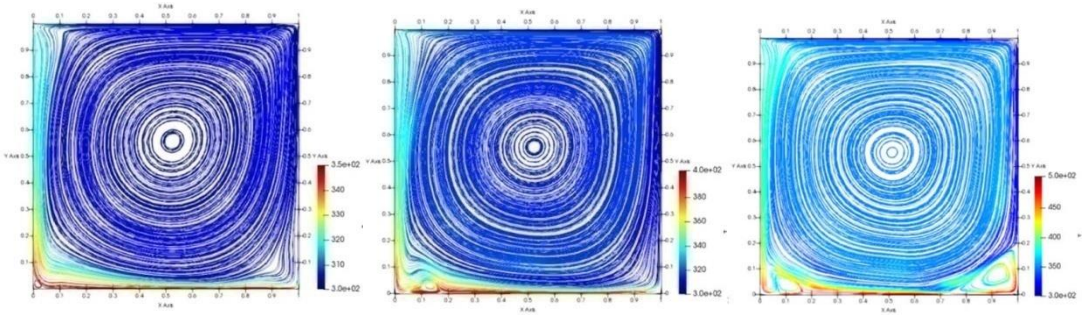

Fig:- Snapshot of Instantaneous Temperature distribution with streamlines inside the cavity at Ri=0, Ri=0.4, Ri=0.8, Ri=1, Ri=2, Ri=4

The temperature contour with streamline from Ri=0 to Ri=4 for Re=1000 is shown above. In these cases, shear roll is dominating inside the cavity and it is a clockwise vortex. Beside this shear vortex, one anticlockwise vortex is also formed in left side of the bottom plate from Ri=0 to Ri=1 which have now disappeared in case of Ri1 and Ri=2. A secondary vortex on right bottom side of the cavity have now emerged in case of Ri=4. Temperature variation inside the cavity is also shown which shows that at the core temperature variation is negligible and fluid inside the cavity is not well mixed in case of Ri=0. As the Richardson number increases from Ri=0 to Ri=4, temperature variation has increased slightly that can be seen inside the shear roll which shows that fluid has now started mixing.

Reynoldsnumber=2500

Ri=0 **Ri=0.4** **Ri=0.8**

Ri=1 **Ri=2** **Ri=4**

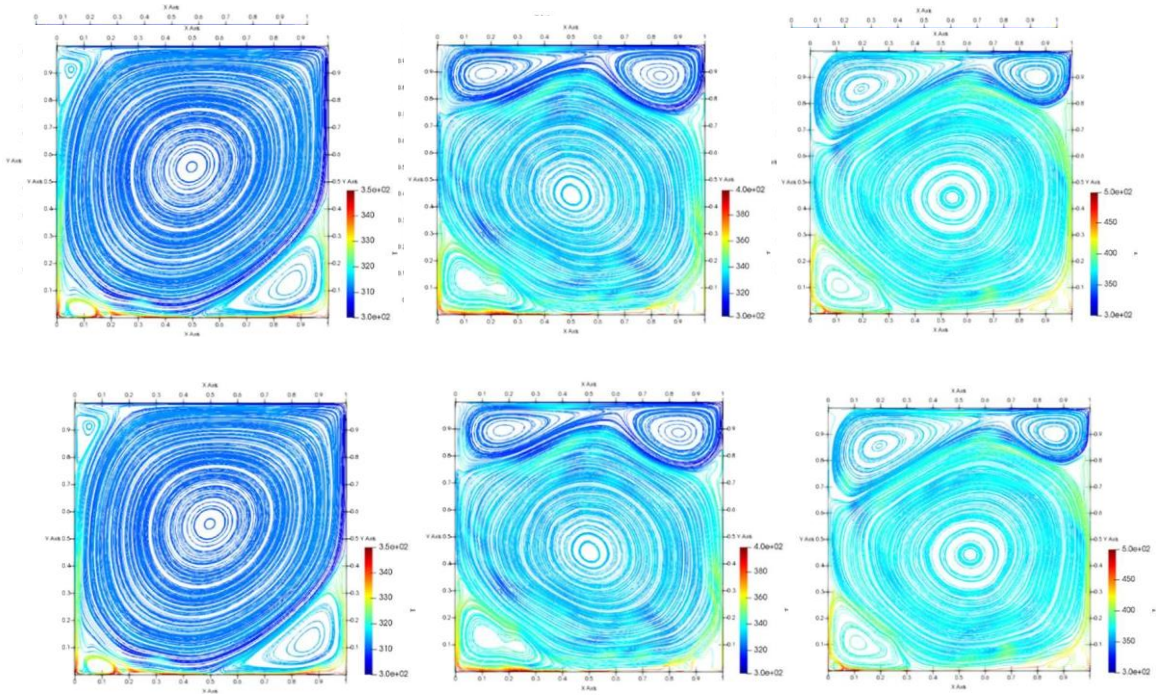

Fig:Snap shot of Instantaneous Temperature distribution with streamlines inside the cavity at Ri=0,Ri=0.4,Ri=0.8,Ri=1,Ri=2,Ri=4

The temperature contour with streamline from Ri=0 to Ri=4 for Re=2500 is shown above. In these cases, shear roll is dominating inside the cavity and it is a clockwise vortex at Ri=0. Beside this shear vortex, one anticlockwise vortex is also formed in left side and one at right side of the bottom plate at Ri=0. Now in case of Ri=0.4 buoyancy roll have started to emerge and the size of shear roll decreases. As we look at the contours of Ri=2 and Ri=4 buoyancy roll is dominant over the shear roll and the temperature inside the buoyancy roll increases. Here the shear roll is submissive and have almost divided into two secondary vortices which can be seen on left and right side of the top plate.

Reynoldsnumber=5000

Ri=0 **Ri=0.4** **Ri=0.8**

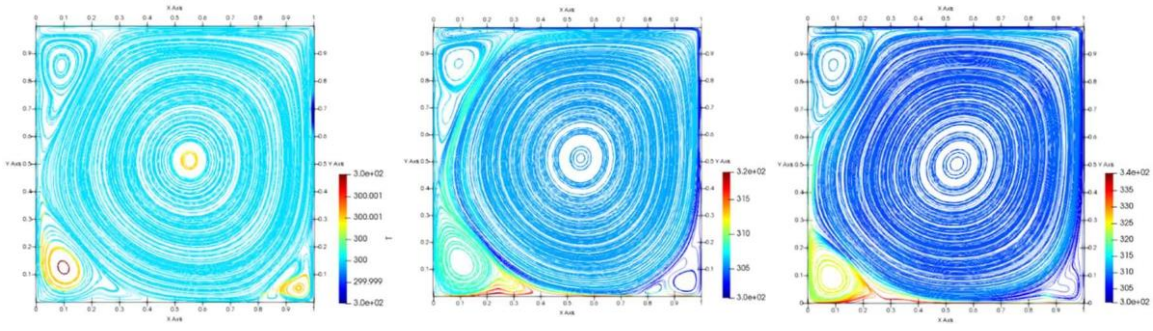

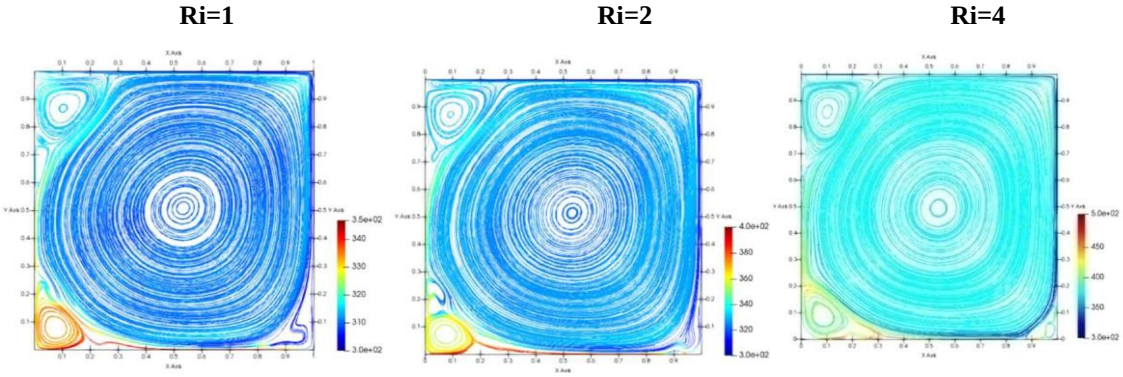

Fig:Snap shot of Instantaneous Temperature distribution with streamlines inside the cavityatRi=0,Ri=0.4,Ri=0.8,Ri=1,Ri=2,Ri=4

The temperature contour with streamline from Ri=0 to Ri=4 for Re=5000 is shown above. Here, beside the buoyancy roll three anti-clockwise vortices are formed out of which two vortices appear on the left and right side of the bottom plate and one anti-clockwise vortex appears on the left side of the top plate. There is slightly increase in the temperature variation inside the secondary vortices placed. The buoyancy roll is dominating here and a significant amount of increase in temperature variation inside the core can be seen from the above contours. Moreover, the secondary vortex on right side of the bottom plate have started to disappear as the Richardson number increases from Ri=0.4 to Ri=4.

Reynoldsnumber=10000

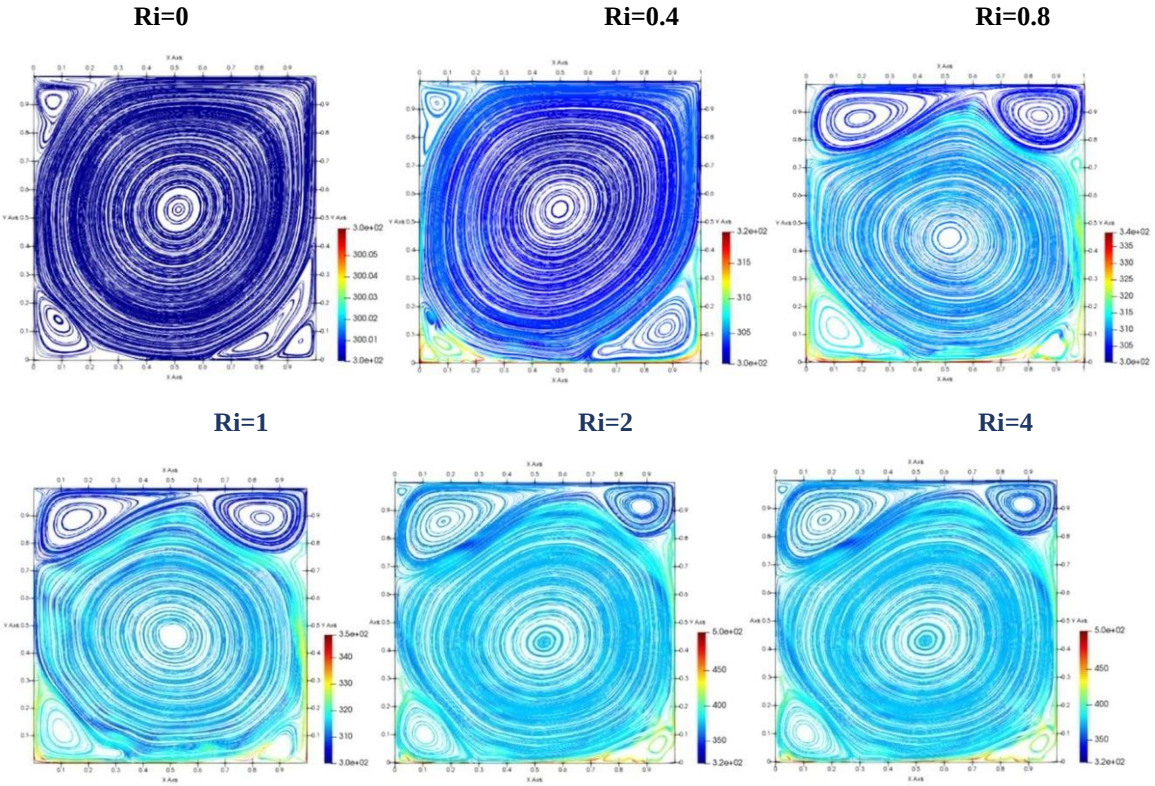

Fig:Snap shot of Instantaneous Temperature distribution with streamlines inside the cavity atRi=0,Ri=0.4,Ri=0.8,Ri=1,Ri=2,Ri=4

The temperature contour with streamline from Ri=0 to Ri=4 for Re=10000 is shown above. Here, the shear roll which is a clockwise vortex is dominating inside the cavity for first two cases of Ri=0 and Ri=0.4. Beside this

shear vortex, three anticlockwise vortices are also formed out of which two vortices arepresent on left and right side of the bottom plate and the third one at left side of the top plate. From the contours of Ri=0.8, 1, 2 and 4 it can be clearly seen that the buoyancy roll have now been dominating over the shear roll as the size of the buoyancy roll increases with reduction in size of shear roll which appears to be divided into two vortices but have not been divided yet. Beside this the size of the vortex present on the right side of the bottom plate have decreased in size.

5. Time Averaged Drag

For Re=500, 1000, 10000 drag experienced by the top plate with respect to time is reported here for Ri = 0, 0.4, 0.8, 1, 2, 4, 5, 6, 10, 11, 1, 13, 15, 16, 25, 30, 35, 50,54, 55, 56, 60, 64, 70, 80, 90, 100. For these cases, we have calculated the time-averaged drag. And finally variation of time-averaged drag with Richardson Number for respective Reynolds number is shown below

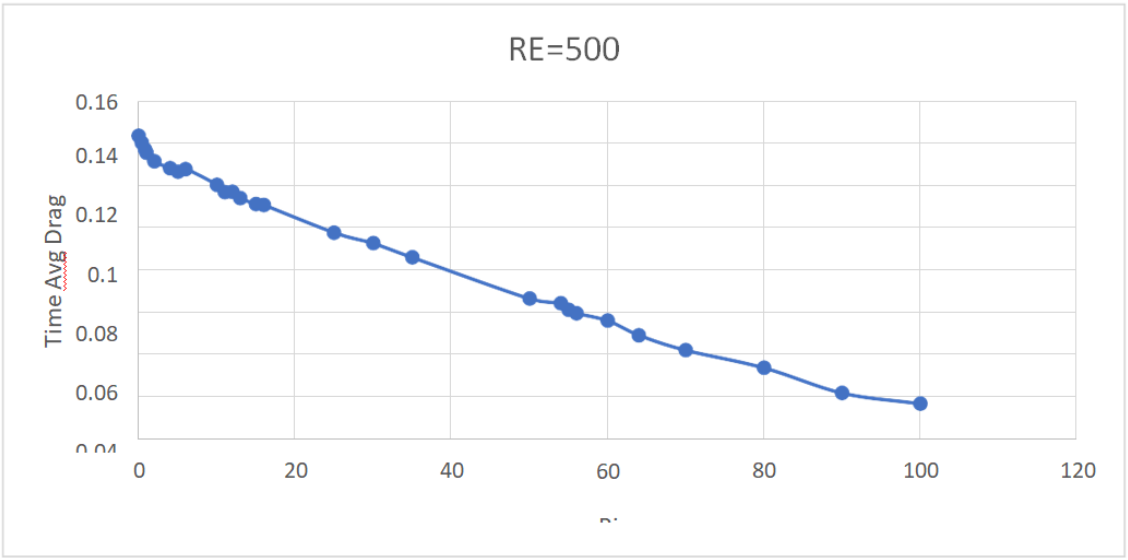

Fig4.3.1:-Riv/sTimeavgdrag(Re=500)

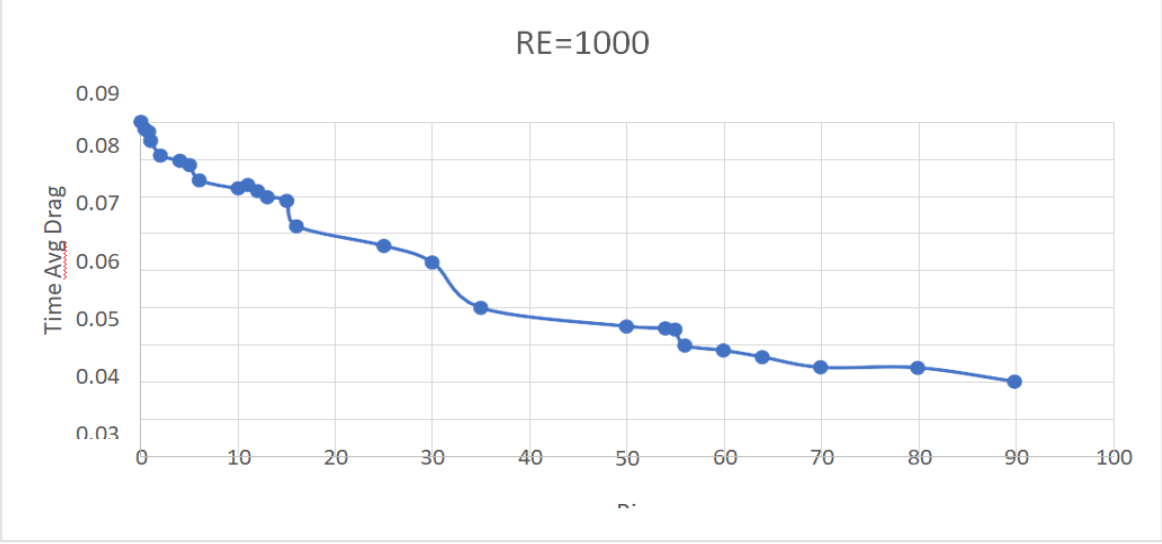

Fig4.3.2:-Riv/sTimeavgdrag(Re=1000)

Above are the Charts for Richardson number v/s Time avd drag for Re=500 and Re= 1000. As the Richardson number increases drag on the plate decreases and becomes minimum at Ri=100 for both of the respective Reynolds numbers. Almost a linear dip for the values of time-avg drag can be seen in case of Re=500.

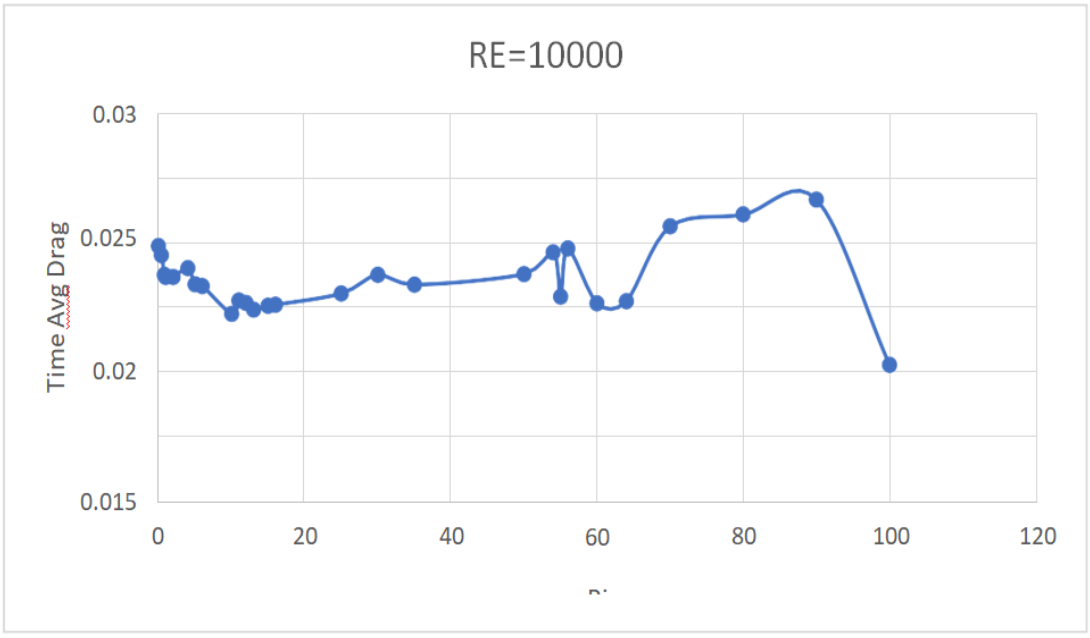

Fig4.3.3:-Riv/sTimeavgdrag(Re=10000)

In case of Re=10000, drag decreases initially up to Ri=10, then increases at Ri=54 and then again decreases uptoRi=60 and Ri=64. Here the value of drag on the plate is maximum at Ri=90 and minimum at Ri=100.

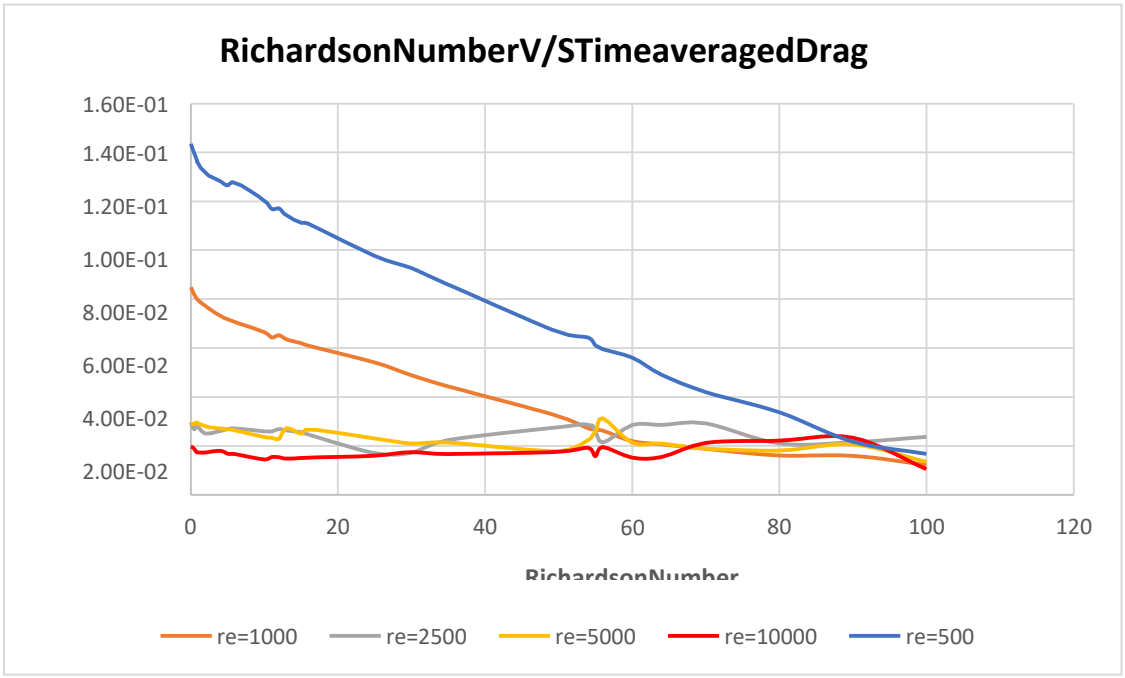

Fig4.3.4:-Riv/sTimeavgdrag(Re=500,1000,2500,5000,10000)

From the above plot it can be justified that buoyancy flow inside the cavity is dominant as we increases the Richardson numbers.

6. Conclusion

In this research paper, a numerical simulation and investigation of different Fluid in a lid-driven cavity were conducted to understand the flow behavior, heat transfer characteristics, and Mixed convective flow in a lid-driven cavity at Re=500,1000,2500,5000 and 10000 has been analyzed numerically. Behavior of fluid flow, streamline patterns with temperature vaariation inside the lid-driven was studied in detail. Close observations of the streamline diagrams reveals that between a certain ranges of Richardson number two vortices inside the cavity always rotates in the clockwise direction. The reason for this behavior is shear and buoyancy effect. In the present study, the shear roll due to the motion of the top plate was dominant in all the cases of Re=500 and Re=1000 whereas, in case of Ri=0.4 at Re=2500 buoyancy roll due to heating of the bottom plate have started to emerge significantly and became dominant over the shear roll for Ri=2 at Re=2500. Moreover, capturing the flow physics whether the flow is steady, chaotic or periodic in nature has been studied in detail which is one of the aim of this work. The main conclusion reached in the present study is about the effect of time averaged drag acting on the top plate with respect to different Richardson numbers ranging from 0 to 100 at Re=500,1000,2500,5000 and 10000. It was concluded that, as the Reynolds number increases, the initial values of drag acting on the plate decreases. The flow inside the cavity is laminar at Re=500 and Re=1000, the drag acting on the upper plate decreases almost linearly and becomes minimum at Ri=100 for the respective cases whereas, in case of Re=2500, 5000 and 10000 a variation can be seen for the values of time-avg drag with respect to richardsonnumber.From the above plot it can be justified that buoyancy flow inside the cavity is dominant as we increases the richardson numbers.

References

[1] P.Le.Quere and T.Alziary De Roqufort “Computation of Natural convection intwodimensionalcavitieswithChebyshevpolynomials”journalofComputationalPhysics(1985)”.

[2] CesarA.CardenasR.etal“OpenFOAMNumericalSimulationswithDifferentLidDrivenCavityShapes(2020)” .Koseff,J.etal."Thelid-drivencavityflow:asynthesisofqualitativeandquantitativeobservations."(1984):390-398).

[3] Quéréetal."Natural-convectionflowsinair-filled,differentiallyheatedcavitieswithadiabatichorizontalwalls." NumericalHeatTransfer,PartA:Applications50.5(2006):437-466.

[4] Venkatadri, K., et al. "Numerical simulation of lid-driven cavity flow of micropolarfluid." IOP Conference Series: Materials Science and Engineering. Vol. 402. No. 1. IOPPublishing,(2018).

[5] Moallemi,M.K.,andK.S.Jang."Prandtlnumbereffectsonlaminarmixedconvectionheattransferinalid-drivencavity."InternationalJournalofHeatandMassTransfer35.8(1992):1881-1892.

[6] Thaker, A. Jignesh P., and B. Jyotirmay Banerjee. "Numerical simulation of flow inlid-drivencavityusingOpenFOAM." Internationalconferenceoncurrenttrendsintechnology: NUiCONE-2011. Ahmedabad: Institute of Technology, Nirma University.(2011).

[7] Ajay dev singh “Numerical simulation of mixed convection in a lid-driven cavity (IITDelhi)(2018).

[8] DigbijoyMukherjee“Numericalsimulationofmixedconvectioninalid-drivencavity(IITDelhi)(2020).

[9] Abanoub G. Kamel and Eman H. Haraz “Numerical simulation of three-sided lid-driven square cavity” journals of Wiley (2020).

[10] L. Jahanshaloo, N. A. CheSidik* and S. Salimi "Numerical Simulation of High Reynolds Number Flow in Lid-Driven Cavity Using MultiRelaxation Time Lattice Boltzmann Method" journals of Advanced Research in Fluid Mechanics and Thermal Sciences (2016), 2289-7879.

[11] KerimYapici a and Bulent Karasozenb" Finite volume simulation of viscoelastic laminar flow in a lid-driven cavity" journals of ELESEVIER (2009).

[12] JagramKushwah and K. C. Arora "CFD Simulation of Lid Driven Cavity Flow" journals of International Journal for Scientific Research & Development (2015), 2321-0613.

[13] Ke Wu, Bruno D. Welfert and Juan M. Log ex "Complex dynamics in a stratified lid-driven square cavity flow" journals of Fluid Me h. (2018).
[14] Carlos Henrique Marchi and Roberta Suero "The Lid-Driven Square Cavity Flow: Numerical Solution with a 1024 x 1024 Grid" journals of ABCM (2009).
[15] By J. - L. G U E RM O N D1, and C. M I G E O N "Start-up flows in a three-dimensional rectangular driven cavity of aspect ratio 1:1:2 at Re = 1000" journals of J. Fluid Mech (2002) vol 450.
[16] U.Ghia, K. N. Ghia, and C. T. Shin, “High-Re Solutions for Incompressible FlowUsing the Navier-Stokes Equations and a Multigrid Method”, Journal of ComputationalPhysics,vol.48,pp.387-411,(1982)”.
[17] O. BOTELLA and R. per et "BENCHMARK SPECTRAL RESULTS ON THE LID-DRIVEN CAVITY FLOW" journals of Pergamon Elsevier (1998). PII: S0045-7930(98)00002-4.
[18] C. S. N. Azwadi*, A. Rajab and A. Sofianuddin "FOUR-SIDED LID-DRIVEN CAVITY FLOW USING TIME SPLITTING METHOD OF ADAMS-BASHFORTH SCHEME " journals of International Journal of Automotive and Mechanical Engineering (IJAME) in (2014).
[19] J. R. Koseff and R. L. Street "The Lid-Driven Cavity Flow: A Synthesis of Qualitative and Quantitative Observations" journals of ASME (1984).
[20] A. Liberzon, Yu. Feldman and A. Yu. Gelfgat "Experimental observation of the steady – oscillatory transition in a cubic lid-driven cavity" journals of Aviv, 69978.